International Journal of Concrete Structures and Materials

RESEARCH

Open Access

Evaluation of the KDS 14 Draft Design Method for Predicting the Shear Strength of Prestressed Concrete Beams

Ngoc Hieu Dinh[1], Si-Hyun Kim[1] and Kyoung-Kyu Choi[1*]

Abstract

One-way shear strength evaluation is one of the essential and complex aspects in the design of prestressed concrete (PSC) members. Current design standards adopt different empirical or semi-empirical approaches to predict the one-way shear strength of PSC members. This study evaluated the applicability of the KDS 14 draft design method, which is based on compression zone failure theory, for predicting the shear strength of slender PSC beams. The evaluation utilized the ACI-DAfStb database, comprising 331 one-way shear tests on PSC beams with and without shear reinforcement. The strength prediction of the KDS 14 draft model was compared against those of existing design codes and design-oriented models. Results indicated that the KDS 14 draft model demonstrated promising performance in predicting the shear strength of a large dataset of PSC beams, both with and without stirrups. For PSC beams without stirrups, the KDS 14 draft model exhibited better accuracy with less scatteredness compared to the ACI 318-19 and CSA A23.3:24 models, while maintaining design conservatism. For PSC beams with stirrups, the KDS 14 draft model showed predictive performance comparable to the CSA A23.3:24 model. In addition, the KDS model exhibits similar scatteredness compared to the mechanics-based model proposed Marí et al. but while providing more conservative predictions. Furthermore, parametric study and design example were conducted to understand the influence of key design parameters and the applicability of the KDS 14 draft model for PSC beams. Overall, the predictions by the KDS 14 draft model closely aligned with trends observed in experimental results across most scenarios.

Keywords Shear strength, Prestressed concrete, Concrete beam, Compression zone, Stirrups

1 Introduction

Prestressed concrete (PSC) beams and girders are structural elements designed to support greater loads and spans compared to traditional reinforced concrete (RC) beams. By incorporating high-strength steel tendons within the concrete, PSC beams undergo pre-compression, counteracting tensile stresses that would otherwise lead to premature cracking. This technique enhances durability and serviceability by altering stress and strain distributions, increasing the cracking load, and refining crack patterns. Shear strength in prestressed concrete beams is particularly noteworthy, which refers to the beam's ability to resist shear forces that could cause failure along diagonal planes. Prestressing forces enhance shear resistance by improving cracking resistance and increasing the effective depth of the beam, making PSC beams and girders ideal for a wide range of construction applications, including bridges and high-rise buildings.

The shear strength of ordinary reinforced concrete beams has been extensively studied over the past few decades through both experimental and analytical

Journal information: ISSN 1976-0485 / eISSN 2234-1315.

*Correspondence:
Kyoung-Kyu Choi
kkchoi@ssu.ac.kr
[1] School of Architecture, Soongsil University, 369 Sangdo-Ro, Dongjak-Gu, Seoul 153-743, South Korea

approaches. Existing literature indicates that shear strength is primarily influenced by several design parameters, including: (i) the shear-span-to-depth ratio (a/d), (ii) concrete compressive strength, (iii) flexural reinforcement ratio, (iv) axial compression or tension force, (v) shear reinforcement ratio, and (vi) member depth. Kani et al. (1964) and Megahed et al. () reported that a decrease in the a/d ratio leads to an increase in shear strength, particularly when the a/d ratio is less than 2.4. Similarly, studies by Johnson et al. (1989) and Perera et al. (2013) demonstrated a general increase in shear strength with higher concrete compressive strength; however, a decline was observed when the concrete strength exceeded 70 MPa. Furthermore, previous research has identified a reduction in shear strength per unit cross-sectional area with increasing member depth, commonly referred to as the size effect (Chen & Zhu, 2024; Dinh et al., 2021; Elsamak et al., 2024; Hassan & Yousif, 2024; Jumaa & Yousif, 2019; Leonhardt & Walther, 1962; Muhammad & Yousif, 2023; Park et al., 2021; Pham et al., 2023; Taylor et al., 1972).

Understanding one-way shear strength is essential for structural design and assessment of PSC members. Since the 1950s, extensive experimental investigations have been undertaken to examine the influence of critical parameters on the shear strength and failure modes of PSC beams and girders. Early studies by Zwoyer and Siess (1954), Hanson and Hulsbos (1964), Kar (1968), and Hegger and Görtz (2003) highlighted that critical design parameters such as the shear span-to-effective depth ratio, concrete compressive strength, prestressing level, longitudinal and shear reinforcement ratios, and cross-sectional shape significantly influence the shear strength of PSC beams. Tao and Du (1985) found that increasing the post-tensioning tendon ratio and longitudinal reinforcement ratio shifted the failure mode of PSC beams from ductile to non-ductile, despite an increase in load-carrying capacity. Research by Elzanaty and Nilson (1986) and Choulli et al. (2008), which focused on PSC beams made with high-strength concrete, indicated a reduction in shear strength compared to beams made with conventional concrete. These findings led to recommendations for limiting the concrete compressive strength to around 65 MPa when calculating shear strength. Rupf et al. (2013) examined post-tensioned I-beams with draped tendons and minimal shear reinforcement, showing that shear strength and failure modes were significantly affected by the quantity of shear reinforcement, the level of post-tensioning force, and the presence of flanges. Similarly, De Silva et al. (2006) investigated the impact of longitudinal and transverse reinforcement ratios, prestressing levels, and concrete strength on crack width and spacing in partially prestressed concrete members. Thoma and Fischer (2023) conducted an experimental investigation into the shear strength of prestressed concrete (PSC) girders with varying amounts of longitudinal reinforcement. This study indicated that a reduced amount of longitudinal reinforcement did not adversely affect the shear capacity if the initial strain of prestressed tendons was increased moderately. Additionally, digital image correlation (DIC) analysis suggested that load-bearing contributions attributed to aggregate interlock may not be appropriate for PSC beams with low ratios of shear reinforcement.

Several prior efforts have contributed to the development of analytical models for predicting the shear strength of PSC beams, which form the basis of the current shear design provisions. Collins et al. (2008) proposed a theoretical model for shear strength prediction of prestressed concrete members with and without shear reinforcement. The model integrated a strut-and-tie approach for disturbed regions and a sectional model for flexural regions. The model was capable of predicting the shear strength of PSC members with high reliability and provided a deep understating regarding the shear stress transfer mechanism. Park et al. (2013) introduced an analytical approach based on the strain-based shear strength model to predict the shear strength of both ordinary and PSC beams. This method assumes that the shear force acting on the beam is primarily resisted by the intact compression zone within the cross-section. The results indicated that the proposed model provided reasonably accurate predictions when compared with existing test data for simply supported PSC beams. Furthermore, the model effectively interprets the influence of various design parameters on the shear strength of prestressed concrete beams. In studies by Zhang et al., (2014a, 2014b), a mechanics-based segmental approach was proposed to predict the presliding shear capacity of PSC beams with or without shear reinforcement. This model is based on the mechanics of partial interaction, which is the slip between reinforcement and surrounding concrete allowing for crack formation and widening to construct the presliding shear failure criteria. Marí et al. (2016) proposed a mechanical model based on the principles of concrete mechanics and assumptions based on the experimental results for predicting the shear-flexural strength of ordinary and PSC beams. In this model, the critical crack in prestressed members is assumed to initiate at a cross-section where the bending moment is comparable to the cracking moment, which occurs further from the zero bending moment point compared to ordinary reinforced concrete members. The predictions obtained by this model demonstrated good agreement with the ACI-DAfStb database consisting of

the test results of 1285 beams with and without shear reinforcement, covering a wide range of geometric characteristics (rectangular, I, or T sections). In addition, design examples were provided to show the practical applicability of the model.

For practical design and performance assessment, current design standards use empirical or semi-empirical equations to predict the one-way shear strength of reinforced concrete members, including PSC beams. In general, the overall shear strength of a member is considered to be the sum of the contributions of the concrete section (V_c) and stirrups (V_s). Table 1 summarizes the design equations of V_c according to existing design codes. In Eurocode 2 (2002), the shear strength equations do not distinguish between ordinary and PSC beams. This standard adopted an empirical approach for a cracked section to derive the design formula from the elastic stress distribution taking into account the axial force acting on the uncracked section. The Canadian Standards CSA A23.3:24 (CSA, 2024) and CSA S6:19 (CSA, 2019), the AASHTO LRFD Bridge Design Specifications (AASHTO, 2024) issued by the American Association of State Highway and Transportation Officials, and the fib Model Code 2010 (fib, 2010) issued by the Euro-International Concrete Committee are based on the modified compression field theory (MCFT) developed by Vecchio and Collins (1986). In this approach, the key design parameters include the concrete contribution factor (β) and the angle (θ) of diagonal compression field, determined by the strain (ε_s) developed in longitudinal tension reinforcement under a given bending moment, shear force, axial force, and prestress. Explicit expressions for β and θ were also provided in these design codes. In the ACI 318-19 (ACI, 2019) code by the American Concrete Institute (ACI), the one-way shear design provisions distinguish between ordinary reinforced concrete and prestressed concrete members. ACI 318-19 offers two methods for calculating V_c for PSC members: a detailed method and an approximate method, both semi-empirical and calibrated

Table 1 Summary of shear strength design models for PSC beams

Models	Shear strength equations for concrete contribution	Shear strength equations for stirrup contribution
ACI 318-19 (2019)	$V_c = \min(V_{ci}, V_{cw})$ $V_{ci} = 0.05\lambda\sqrt{f'_c}b_w d_p + V_d + \frac{V_i M_{cre}}{M_{\max}} \geq V_{ci,\min}$ $M_{cre} = \left(\frac{I}{y_t}\right)(0.5\lambda\sqrt{f'_c} + f_{pe} - f_d)$ $V_{cw} = (0.29\lambda\sqrt{f'_c} + 0.3f_{pc})b_w d_p + V_p$ $V_{ci,\min} = 0.14\lambda\sqrt{f'_c}b_w d \quad for \ A_{ps}f_{se} < 0.4(A_{ps}f_{pu} + A_s f_y)$ $V_{ci,\min} = 0.17\lambda\sqrt{f'_c}b_w d \quad for \ A_{ps}f_{se} \geq 0.4(A_{ps}f_{pu} + A_s f_y)$	$V_s = \frac{A_v f_{yv} d}{s}$
CSA A23.3:19 (2019)	$V_c = \phi_c\lambda\beta\sqrt{f'_c}b_w d_v$ $d_v = \max(0.9d,\ 0.72h)$ $\beta = \frac{0.4}{(1+1500\varepsilon_x)} \cdot \frac{1300}{(1000+s_{ze})} \leq 0.05,$ $\varepsilon_x = \frac{M_f/d_v + V_f - V_p + 0.5N_f - A_p f_{po}}{2(E_s A_s + E_p A_p)}, \quad -0.0002 \leq \varepsilon_x \leq 0.003$ $s_{ze} = \frac{35 s_z}{15 + a_g} \geq 0.85 s_z$	$V_s = \frac{\phi_s A_v f_{yv} d_v}{s}\cot\theta$ $\theta = 29 + 7000\varepsilon_x,$ $30^o \leq \theta \leq 60^o$
KDS 14 draft model (2024)	$V_c = \lambda k_s f_{te} b_w c_u \sqrt{1 + f_{cc}/f_{te}}$ $k_s = 0.75 \leq \sqrt[4]{300/d} \leq 1.1$ $c_u = \left(\frac{P_{b0}}{\varepsilon_c E_c} - \sum n_s A_{s,i} - \sum n_p A_{p,i} + \sqrt{\left(\frac{P_{b0}}{\varepsilon_c E_c} - \sum n_s A_{s,i} - \sum n_p A_{p,i}\right)^2 + 2b_w\left(\sum n_s d_{s,i} A_{s,i} + \sum n_p d_{p,i} A_{p,i}\right)} \right) \Big/ b_w$ $n_i = E_s(\text{or } E_p)/E_c,\ f_{te} = 0.2\sqrt{f'_c},$ $f_{cc} = \frac{M_{ud} + \sum\left[P_{p,i} - A_{p,i}\frac{(d_{p,i} - c_u)}{c_u}\varepsilon_c E_p\right](d - d_{p,i}) - \sum A_{s,i}\frac{(d_{s,i} - c_u)}{c_u}\varepsilon_c E_s (d - d_{s,i})}{b_w c_u (d - \frac{c_u}{3})} \leq \frac{2}{3}f'_c \ M_{ud} = 0.75M_u + \sum P_{p,i}(d_{p,i} - h/2) \geq 1.5M_{cr}$	$V_s = \frac{A_v f_{yv} d}{s}$
Laskar et al. (2010)	$V_c = \frac{1.17}{(a/d)^{0.7}}\sqrt{f'_c}b_w d$	$V_s = \frac{A_v f_{yv} d}{s}$
Marí et al. (2016)	$V_c = \zeta\frac{c}{d}K_p\left[0.3\frac{f'^{2/3}_c}{\gamma_c} + 0.5\left(1 + \frac{b}{b_w}\right)\frac{V_s}{bd}\right]b_{v,eff} d$ $\frac{c}{d} = \frac{c_0}{d} + \left(\frac{h}{d} - \frac{c_0}{d}\right)\left(\frac{d}{h}\right)\frac{\sigma_{cp}}{\sigma_{cp} + f_{ct}}$ $\frac{c_0}{d} = n\rho_l\left(-1 + \sqrt{1 + \frac{2}{n\rho_l}}\right),\ n\rho_l = \frac{E_s A_s}{E_c bd} + \frac{E_p A_p}{E_c bd}$	$V_s = (d_s - c)\cot\theta\frac{A_v f_{yv}}{s}$ $\cot\theta = \frac{0.85 d_p}{d_p - c} \leq 2.5$

from existing experimental data. In the detailed method, V_c is calculated as the lesser of web shear strength (V_{cw}) and flexural shear strength (V_{ci}), based on the theoretical background of Morrow and Viest (1957), Sozen and Hawkins (1962), and Kuchma et al. (2008). The size effect coefficient (λ_s) was newly introduced in the ACI 318-19 model.

In reliability analysis and probabilistic performance-based design using current design codes, several studies have developed probabilistic shear strength prediction models to quantify model uncertainties. Liu et al. (2023) assessed the probabilistic error of existing design models for shear strength prediction using a database of 369 PSC girders that failed in shear. Based on this assessment, the Bayesian probabilistic polynomial correction approach was employed to develop probabilistic shear strength models for PSC girders. Furthermore, Liu et al. (2025) extended this work by developing a Gaussian process regression (GPR)-based model for predicting the shear capacity of PSC beams.

Recently, the draft version of the Korean Design Standard, KDS 14 20 22 (KCI, 2024) issued by the Korea Concrete Institute (KCI) adopted the unified shear strength model originally developed by Park et al. (2006) and Choi et al. (2016) to evaluate the one-way shear of ordinary reinforced concrete (RC) members. This model is based on the theory of compression zone failure for beams governed by flexural shear failure mechanism and has shown a strong correlation with a comprehensive database that covers a wide range of design parameters (Choi et al., 2016). Since a PSC beam can be considered to be similar to the case of an ordinary RC beam subjected to the combined action of compressive force and bending moment, the model is expected to be capable of predicting the shear strength of prestressed concrete members.

This study aims to evaluate the applicability of the KDS 14 draft model, which is based on the compression zone failure mechanism, for predicting the shear strength of slender prestressed concrete (PSC) members. Additionally, its predictive performance is compared with those of two state-of-the-art international design codes and two design-oriented models. To achieve this, the ACI-DAfStb database, comprising 331 tests of PSC beams with and without shear reinforcement, was utilized. Furthermore, a parametric analysis and a design example are presented to understand the influence of key design parameters and assess the practical applicability of the KDS 14 draft model to PSC beams.

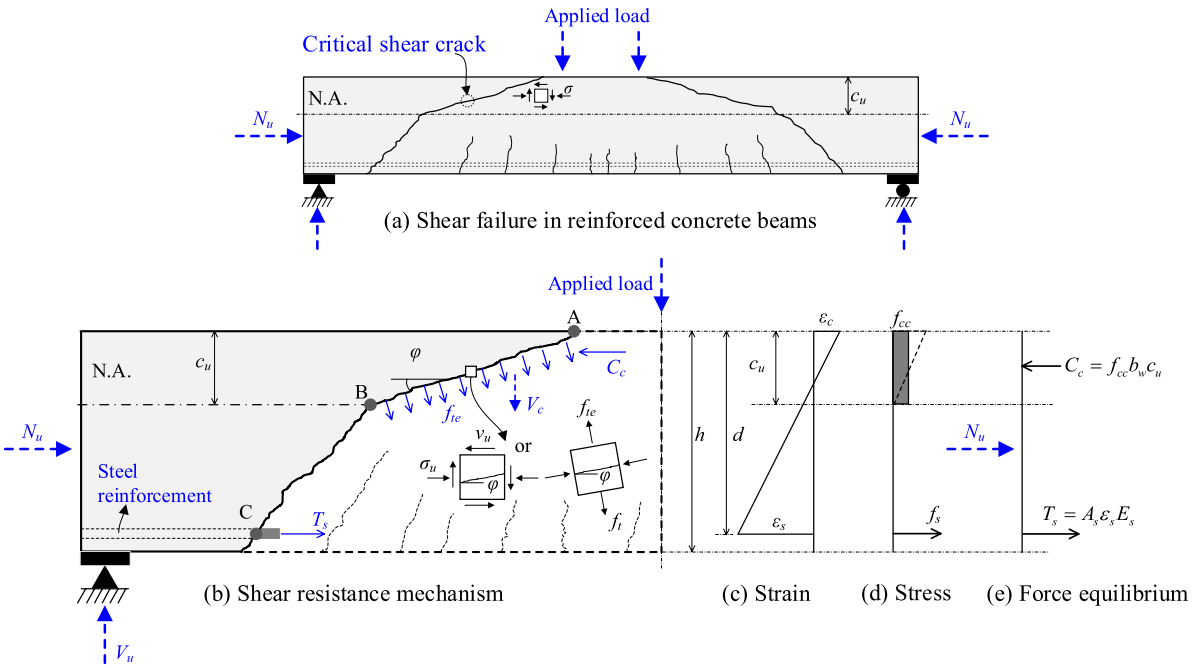

Fig. 1 Shear resistance mechanism of reinforced concrete beams subjected to combined bending and compressive force based on KDS 4 draft design model

2 Review of One-Way Shear Model Based on Compression Zone Failure Mechanism

In the KDS 14 draft model, the one-way shear strength of slender RC members is attributed to the uncracked concrete in the compression zone (Choi et al., 2016). Fig. 1 depicts the shear resistance mechanism and stress state at the shear-critical section within the compression zone of slender RC beams without shear reinforcement, subjected to the combined action of bending moment and concentric axial load. During the initial loading phase, multiple flexural cracks develop within the tension zone of slender beams. As the applied load increases, these flexural cracks propagate toward the beam web and eventually penetrate the compression zone, leading to the formation of critical diagonal macrocracks. At the ultimate loading stage, shear failure occurs within the compression zone (A–B) as it loses its ability to act as a continuum or resist the compressive forces induced by the applied flexural moment. The shear capacity provided by the compression zone can be estimated using the concrete tensile strength, f_{te}, along the critical shear crack within the compression zone:

$$V_c = f_{te}\frac{c_u}{\sin\varphi}b_w\cos\varphi = f_{te}b_w c_u\cot\varphi, \tag{1}$$

where c_u is the depth of the compression zone; f_{te} [$=0.2\sqrt{f'_c}$] is the concrete tensile strength specified in the KDS 14 draft model accounting for biaxial stress state; f'_c is the compressive strength of concrete; b_w is the beam web width; and ϕ is the average angle of inclined crack in the compression zone, is determined based on the principal stress axis using the Rankine failure criterion (Chen, 1982):

$$\cot\varphi = \sqrt{f_{te}(f_{te}+f_{cc})}/f_{te}, \tag{2}$$

where f_{cc} is the average compressive normal stress acting on the compression zone. By substituting Eq. (2) into Eq. (1), the shear contribution of the compression zone for the flexural RC members can be expressed as:

$$V_c = f_{te}b_w c_u\sqrt{1+f_{cc}/f_{te}}. \tag{3}$$

By incorporating the size effect factor (k_s) and reduction factor for lightweight concrete (λ), the final expression for V_c in the KDS 14 draft model is given by:

$$V_c = \lambda k_s f_{te}b_w c_u\sqrt{1+f_{cc}/f_{te}}, \tag{4}$$

where

$$k_s = 0.75 \le \sqrt[4]{300/d} \le 1.1, \tag{5}$$

$$\lambda = \begin{cases} 1.0 \text{ for Normal weight concrete} \\ 0.85 \text{ for Sand - lightweight concrete} \\ 0.75 \text{ for All - lightweight concrete.} \end{cases} \tag{6}$$

In practical design, the depth of the compression zone, c_u, in Eq. (4) can be determined based on the conditions of force equilibrium and strain compatibility at the critical section. These conditions can be expressed as follows under the assumption of a linear distribution of both compressive stress and strain within the compression zone, as illustrated in Fig. 1c–e:

$$C_c = T \text{ or,} \tag{7}$$

$$\frac{1}{2}\varepsilon_c E_c b_w c_u = A_s\varepsilon_s E_s + N_u = \rho_s b_w d\varepsilon_s E_s + N_u, \tag{8}$$

$$\varepsilon_s = \varepsilon_c(d-c_u)/c_u, \tag{9}$$

where C_c is the resultant compressive force of concrete in the compression zone; T_s is the tensile force developed in the tension longitudinal rebars; A_s and E_s are the total cross-sectional area and elastic modulus of the tensile reinforcement, respectively; ρ_s and ε_s are the longitudinal reinforcement ratio and strain in tensile reinforcement, respectively; and ε_c is the allowable concrete compressive strain at the extreme compression fiber at the critical section.

In beams subjected to combined bending and axial load, the compression zone depth is typically higher than that of ordinary beams due to the effect of axial force, and shear failure occurs generally before ε_c reaches the maximum strain ε_0 [$\approx$ 0.002] corresponding to the concrete compressive strength (Choi et al., 2016). Therefore, the KDS 14 draft model adopts a value of $\varepsilon_c = 0.001$ for the shear strength evaluation of PSC members for conservative design.

From Eqs. (7), (8) and (9), the final expression for calculating c_u is obtained as

$$c_u = d\left[\frac{N_u}{b_w d\,E_c\varepsilon_c} - n\rho_s + \sqrt{\left(\frac{N_u}{b_w d\,E_c\varepsilon_c} - n\rho_s\right)^2 + 2n\rho_s}\right], \tag{10}$$

where n [$=E_s/E_c$] is the modulus ratio between steel reinforcement and concrete.

The one-way shear strength in the compression failure mechanism-based model is significantly influenced by the magnitude of the average compressive stress (f_{cc}) acting on the compression zone, as shown in Eq. (4). Under a combined action of factored flexural moment (M_u) at a given design section and axial force (N_u), f_{cc} can be calculated based on the moment equilibrium condition at

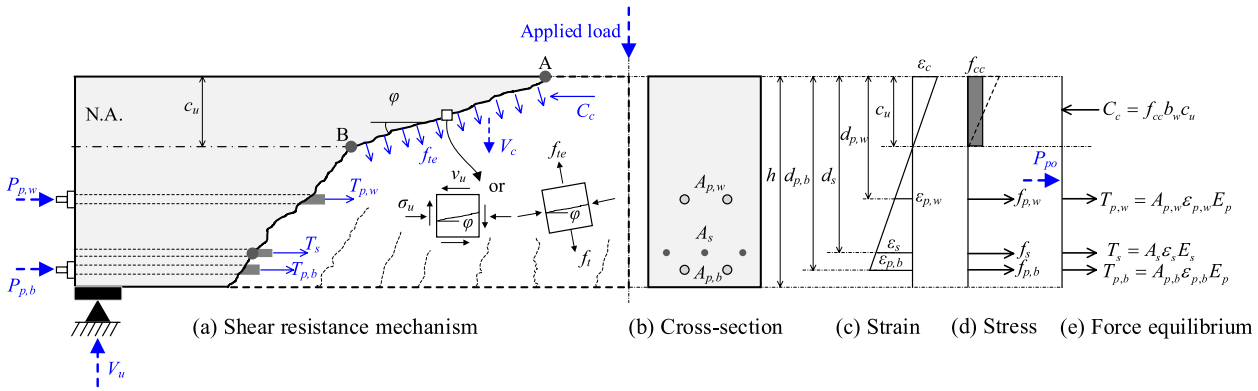

Fig. 2 Shear resistance mechanism of PSC beams based on KDS 4 draft design model

the tensile reinforcement location (see Fig. 1d, e), using the following equation (KDS 14 20 22, 2024):

$$f_{cc} = \frac{M_{ud} + N_u(d - h/2)}{b_w c_u (jd)} \le \frac{2}{3} f_c', \tag{11}$$

where $M_{ud}[= 0.75M_u \ge 1.5M_{cr}]$ is the design-factored flexural moment for conservative design purposes, considering the reduction factor of 0.75, jd $[= d - c_u/3]$ represents the moment arm, which is simply calculated assuming that compressive stress follows a linear distribution in the compression zone, and M_{cr} is the cracking moment (ACI 318-19, 2019).

3 Application of the KDS 14 Draft Model to PSC Beams

The KDS 14 draft model for one-way shear strength was applied to PSC beams. Fig. 2 illustrates the shear resistance mechanism of PSC beams without shear reinforcement, subjected to combined bending moments and prestressing forces. To account for the effects of different reinforcement types (e.g., non-prestressed and prestressed reinforcement), the equivalent effective depth of the beams is defined as follows (Marí et al., 2016):

$$d = \frac{\sum E_s A_{s,i} d_{s,i} + \sum E_p A_{p,i} d_{p,i}}{\sum E_s A_{s,i} + \sum E_p A_{p,i}} \ge 0.8h, \tag{12}$$

where $d_{s,i}$ and $d_{p,i}$ are the distances from the extreme compression fiber to the centroid of the i-th layers of tensile reinforcement and tendons, respectively; and A_s and $A_{p,i}$ are the cross-sectional areas of the tensile reinforcement and tendons, respectively.

At the critical section of PSC beams, force equilibrium and strain compatibility conditions are expressed as follows:

$$\frac{1}{2}\varepsilon_c E_c b_w c_u = \sum A_{s,i}\varepsilon_{s,i} E_s + \sum A_{p,i}\varepsilon_{p,i} E_p + P_{p0}, \tag{13}$$

$$\varepsilon_{s,i} = \varepsilon_c (d_{s,i} - c_u)/c_u, \tag{14}$$

$$\varepsilon_{p,i} = \varepsilon_c (d_{p,i} - c_u)/c_u, \tag{15}$$

where $P_{p0} = \sum P_{p,i}$ is the total prestressing force acting on the beam cross-section after considering stress loss; $E_c = 8500\sqrt[3]{f_c'}$(KDS 14 20 22, 2024) is the elastic modulus of concrete; E_p is the elastic modulus of tendons; and $\varepsilon_{s,i}$ and $\varepsilon_{p,i}$ are the strains in the i-th layer of tensile reinforcement and prestressed tendon, respectively.

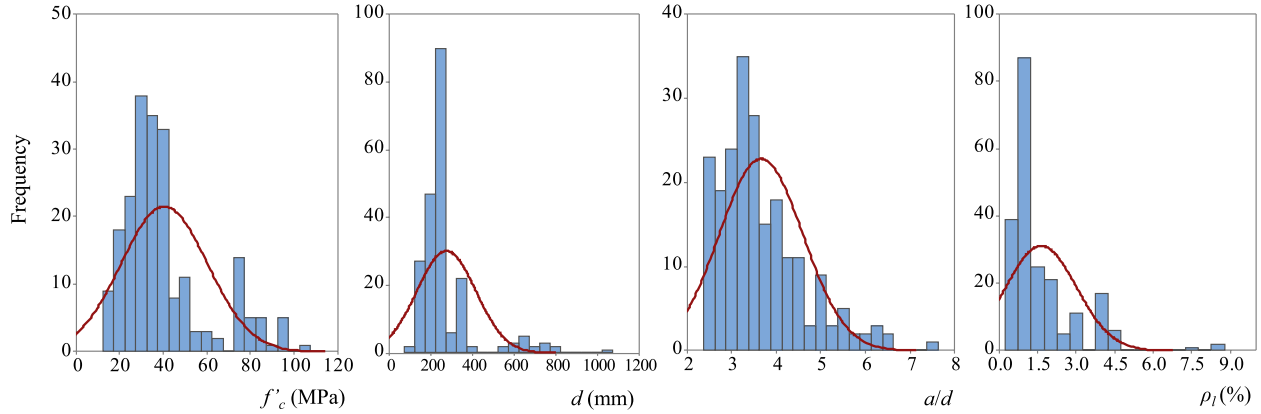

Fig. 3 Distribution of design parameters for database of PSC beams without stirrups

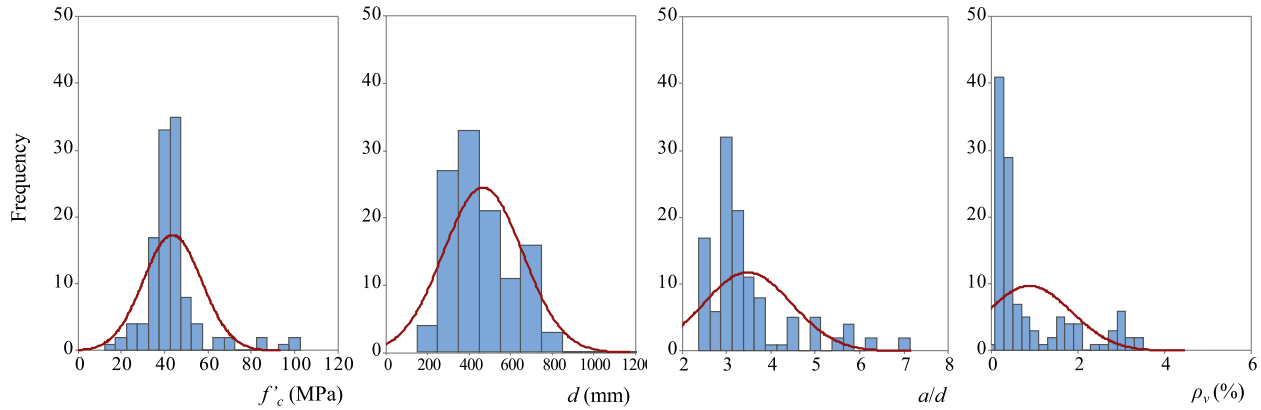

Fig. 4 Distribution of design parameters for database of PSC beams with stirrups

The final expression for the compression zone depth, c_u, in PSC beams can be derived from Eqs. (13–15) by solving a quadratic equation:

$$c_u = \left(\frac{P_{p0}}{\varepsilon_c E_c} - \sum n_s A_{s,i} - \sum n_p A_{p,i} + \sqrt{\left(\frac{P_{p0}}{\varepsilon_c E_c} - \sum n_s A_{s,i} - \sum n_p A_{p,i}\right)^2 + 2b_w \left(\sum n_s d_{s,i} A_{s,i} + \sum n_p d_{p,i} A_{p,i}\right)} \right) / b_w, \quad (16)$$

where $n_s \left[= \frac{E_s}{E_c}\right]$ and $n_p \left[= \frac{E_p}{E_c}\right]$ are the modulus ratios of tensile reinforcement and prestressed tendons, respectively, relative to concrete.

The average compressive stress (f_{cc}) in the compression zone, as shown in Eq. (4), is redefined based on moment equilibrium at the location of equivalent effective depth, considering the effect of prestressed tendons:

$$f_{cc} = \frac{M_{ud} + \sum \left[P_{p,i} - A_{p,i} \frac{(d_{p,i} - c_u)}{c_u} \varepsilon_c E_p\right](d - d_{p,i}) - \sum A_{s,i} \frac{(d_{s,i} - c_u)}{c_u} \varepsilon_c E_s (d - d_{s,i})}{b_w c_u \left(d - \frac{c_u}{3}\right)} \leq \frac{2}{3} f'_c, \quad (17)$$

where M_{ud} is the total applied moment at the design section, calculated as the summation of design-factored flexural moment (M_u) and additional moment caused by the eccentric prestressing force:

$$M_{ud} = 0.75 M_u + \sum P_{p,i}(d_{p,i} - h/2) \geq 1.5 M_{cr}, \quad (18)$$

where $P_{p,i}$ is the prestressing force in the i-th layer of the tendon.

The design equations of the KDS 14 draft model for PSC beams are summarized in Table 1.

4 Database Assessment Using KDS 14 Draft Model and Existing Design Models

4.1 Database of PSC Beam Specimens

A comprehensive ACI-DAfStb database (Dunkelberg & Reineck, 2017) comprising 331 tests on slender PSC beams, with or without shear reinforcement, was used to evaluate the applicability of the KDS 14 draft model. Detailed information on the test specimens is presented in the Appendix (Tables A1, A2). Figs. 3 and 4 present the distribution of specimens in the database according to primary design parameters. For PSC beams without stirrups (Fig. 3), the concrete compressive strength (f'_c) ranged from 13 to 103 MPa, effective depth varied from 109 to 1025 mm, the shear span-to-effective depth ratio (a/d) varied from 2.4 to 7.4, and total tension longitudinal reinforcement ratio (ρ_l) varied from 0.28 to 8.74%. For PSC beams with stirrups (Fig. 4), the concrete compressive strength (f'_c) ranged from 16 to 100 MPa, effective depth varied from 152 to 1360 mm, the shear span-to-effective depth ratio (a/d) varied from 2.5 to 6.9, and shear reinforcement ratio (ρ_w) varied from 0.1 to 3.49%. Moreover, the database included other wide range of parameters, such as cross-sectional shapes (rectangular, I-shaped, and T-shaped) and prestressing methods (pre- and post-tensioned tendons).

4.2 Shear Strength Evaluation Using the KDS 14 Draft Model and Comparison with Existing Design Methods

Two existing state-of-the-art international design guidelines, ACI 318-19 (ACI, 2019) and CSA A23.3:24 (CSA, 2024), and two design-oriented models proposed by Laskar et al. (2010) and Marí et al. (2016) were used for a comparative analysis with the KDS 14 draft model. The details of design equations of the design models are summarized in Table 1. For ACI 318-19 (2019), the detailed method was used. It should be noted that for the evaluation process, material reduction and safety factors in the design equations were set to 1.0 to ensure a consistent comparison.

According to the KDS 14 draft model as presented in Sect. 3, the one-way shear strength of concrete (V_c) varied along the member length due to the variation in the average compressive stress (f_{cc}) caused by the factored flexural moment M_u (refer to Eqs. (17) and (18). Consequently, V_c should be checked along the member length at the potential shear-critical sections during the design process. For the evaluation of shear strength using the database, test specimens were simply supported and subjected to four-point bending until failure. The KDS 14 draft model recommends that the critical shear section should be checked at a distance of 1.2 times the effective depth from the end support ($1.2\times d$). Thus, the total applied moment (M_{ud}) at the critical section, as specified in Eq. (18), can alternatively be determined using the following equation:

$$M_{ud} = (1.2 \times d)V_{test} + \sum P_{p,i}(d_{p,i} - h/2) \geq 1.5M_{cr}, \tag{19}$$

where V_{test} is the shear load at failure obtained from test results.

Moreover, beams in the database exhibited failure modes corresponding to either critical shear or flexure-shear. Therefore, the shear strength (V_n) of the PSC beams should not exceed the shear demand (V_y) corresponding to reinforcement yielding. V_y can be approximated using equivalent rectangular stress block (ACI 318-19, 2019) and force equilibrium condition at flexural yielding:

$$V_n \leq V_y = \frac{M_y}{a} = \frac{\sum A_{p,i}f_{py}(d_{p,i} - \frac{a_f}{2}) + \sum A_{s,i}f_{sy}(d_s - \frac{a_f}{2})}{a}, \tag{20}$$

$$a_f = \frac{\sum A_{p,i}f_{py} + \sum A_{s,i}f_{sy}}{0.85f'_c b_w}, \tag{21}$$

where f_{py} and f_{sy} are the yield strengths of the tendons and tensile reinforcement, respectively; and a_f is the depth of the rectangular stress block.

4.2.1 PSC Beams Without Stirrups

Fig. 5 presents the prediction performance for the data set of PSC beams without stirrups in terms of the shear strength ratio ($V_{test}/V_{predict}$) between test and prediction results, according to different design parameters: concrete compressive strength (f'_c), effective depth (d), a/d ratio, and longitudinal reinforcement ratio (ρ_l). The reliability of the models was assessed using statistical metrics such as the minimum, maximum, and average values, coefficient of variation (COV), and average absolute error (AAE) of the shear strength ratio. The AAE was computed using Eq. (22) as follows:

$$\text{AAE} = \frac{1}{n}\sum_{i=1}^{n}\left|\frac{V_{predict,i} - V_{test,i}}{V_{test,i}}\right|, \tag{22}$$

where n is the number of test specimens used in the statistics and $V_{test,i}$ and $V_{predict,i}$ are the test results and predictions, respectively. AAE is one of the key statistical measures indicating the correlation between the dataset

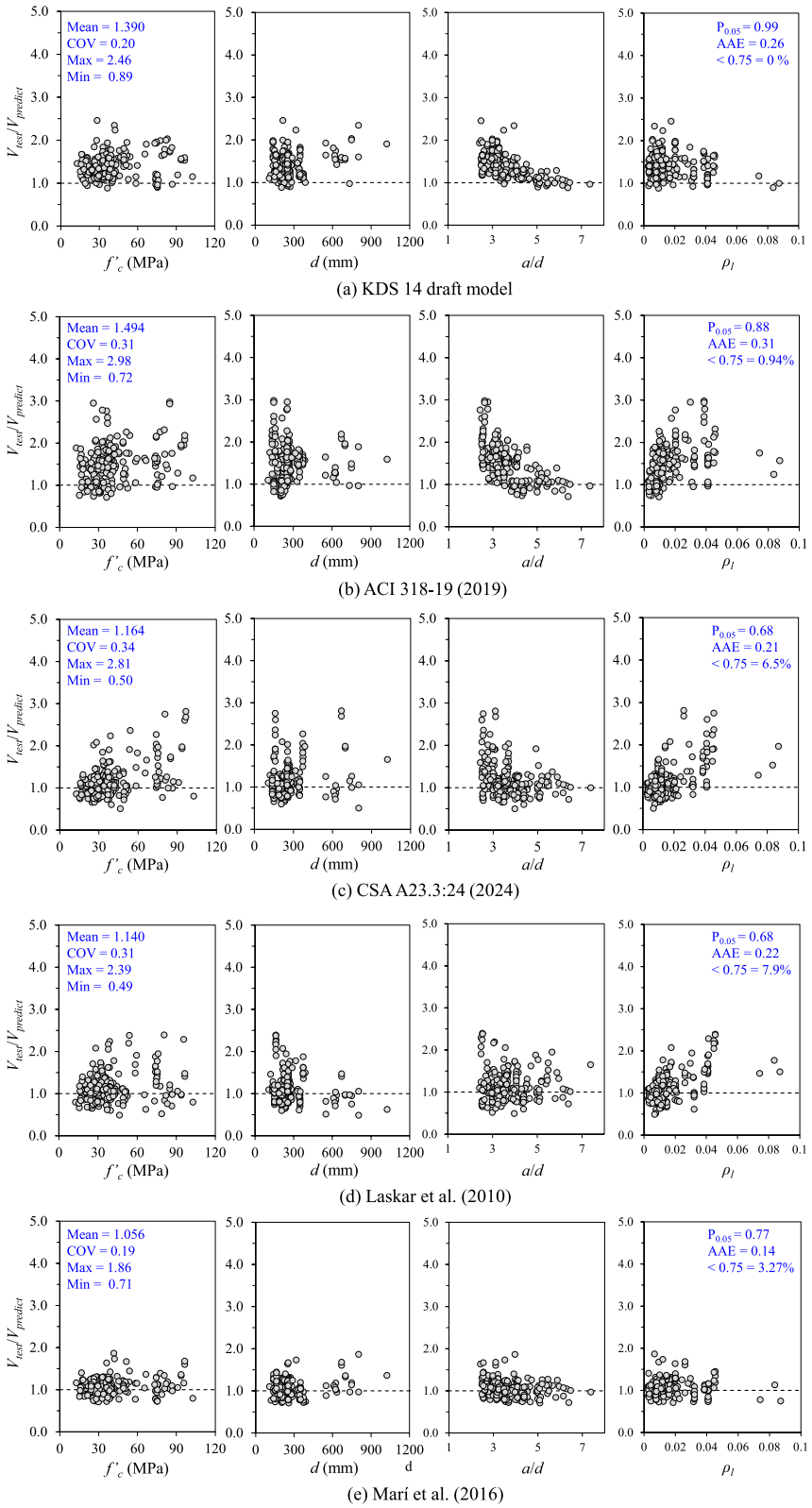

Fig. 5 Comparative analysis of shear strength ratio using different design models for PSC beams without stirrups

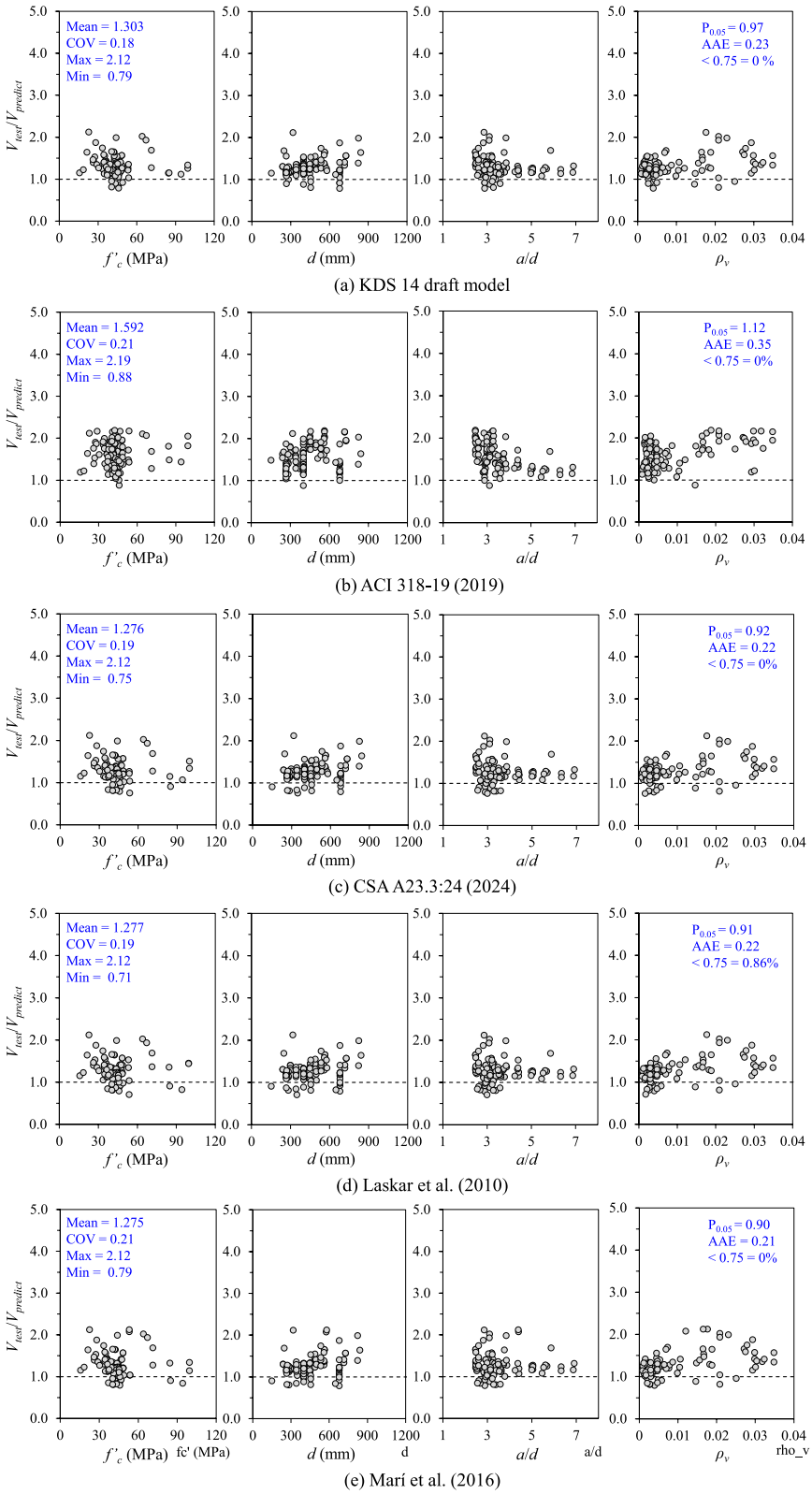

Fig. 6 Comparative analysis of shear strength ratio using different design models for PSC beams with stirrups

of prediction and test results: the lower the AAE value, the better the model correlates with the dataset.

Additionally, the safety of different design equations was further evaluated using the 5% fractile indicator ($P_{0.05}$), assuming a log-normal distribution of the ratio $V_{test}/V_{predict}$ (Liu et al. (2023). The $P_{0.05}$ value is generally accepted as a characteristic value of resistance in the limit state theory (EN1990:2002, 2002): values $P_{0.05}$ closer to 1.0 reflect better safety. Furthermore, the analysis included the percentage of specimens with $V_{test}/V_{predict}$ below 0.75, which corresponds to the strength reduction factor used in shear design.

Overall, all prediction models provided conservative estimates compared to the experimental dataset across various design parameters, as indicated by the low percentage (ranging from 0 to 7%) of specimens with shear strength ratios below 0.75. As shown in Fig. 5a, the KDS 14 draft model exhibited better accuracy and the lowest scatteredness among the models, with a COV of 20%, an AAE of 0.26, and a mean value of $V_{test}/V_{predict}$ of 1.40. The KDS 14 draft model also ensured an acceptable safety level, with zero percentage of specimens exhibiting $V_{test}/V_{predict}$ below 0.75 and a $P_{0.05}$ value of 0.99 (close to the ideal value of 1.0).

The CSA A23.3:24 model (Fig. 5c) yielded a good correlation with test results, achieving a mean $V_{test}/V_{predict}$ ratio of 1.16 and an AAE of 0.21. However, compared to the ACI 318-19 model (Fig. 5b) and the KDS model (Fig. 5a), the CSA A23.3:24 model exhibited a lower safety level, with a $P_{0.05}$ value of 0.68 and the minimum $V_{test}/V_{predict}$ ratio of 0.49. Furthermore, 7% of the specimens evaluated using this model had $V_{test}/V_{predict}$ ratios below 0.75, indicating unconservative predictions in certain scenarios.

Among the two design-oriented models, the mechanics-based model proposed by Marí et al. (Fig. 5e), which accounts for primary shear transfer actions, showed high accuracy when compared with experimental results, yielding a mean $V_{test}/V_{predict}$ ratio of 1.06, an AAE of 0.14, and a COV of 19%. This model also ensures an acceptable

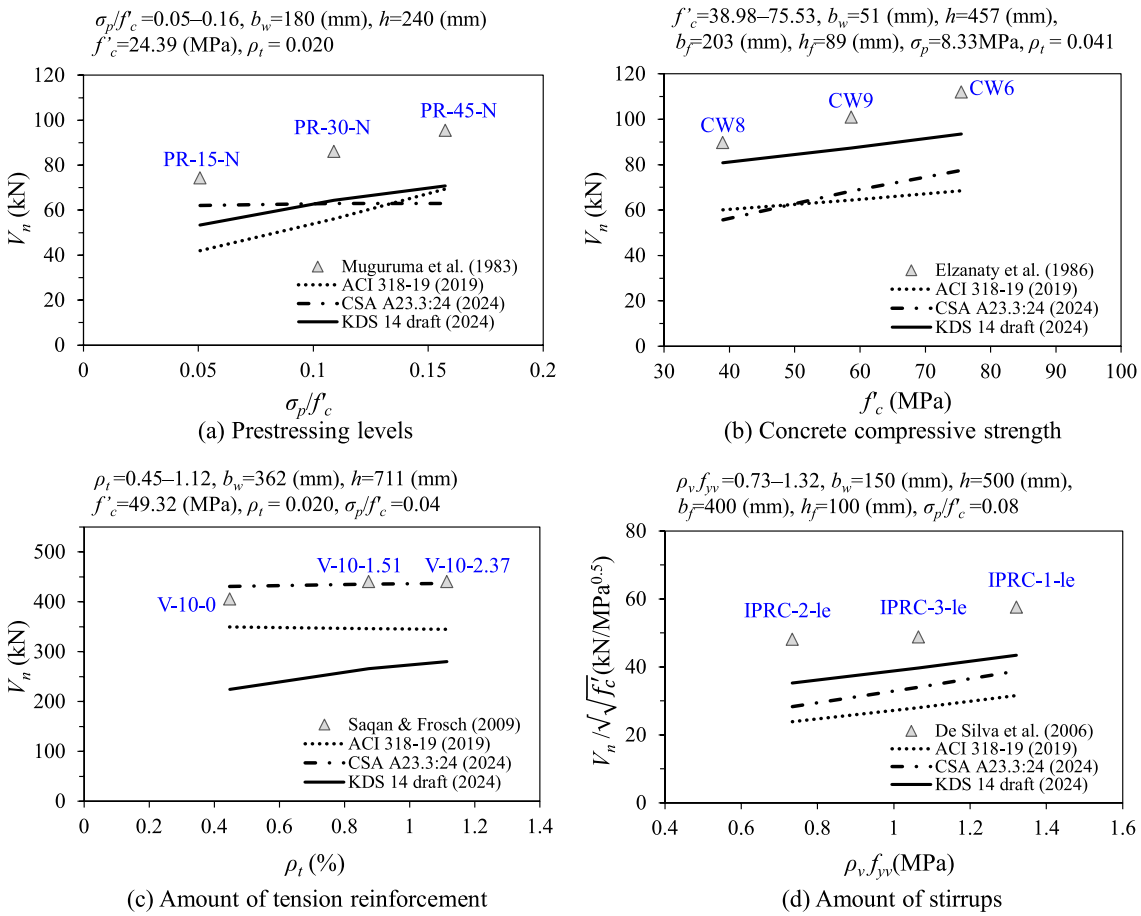

Fig. 7 Parametric study using design models

safety level, as indicated by the small percentage (3.27%) of specimens with $V_{test}/V_{predict}$ ratios below 0.75 and a $P_{0.05}$ value of 0.77. In comparison, the KDS model, which is based on compression zone failure, exhibits a similar level of scatteredness (20%) but provides more conservative predictions.

4.2.2 PSC Beams with Stirrups

Fig. 6 presents a comparative analysis of the shear strength ratio ($V_{test}/V_{predict}$) for the dataset of PSC beams with stirrups, evaluated against various design parameters: concrete compressive strength (f'_c), effective depth (d), a/d ratio, and shear reinforcement ratio (ρ_v). For the PSC beams with shear reinforcement, the shear strength is calculated as the summation of the contribution of concrete (V_c) and stirrup (V_s). Table 1 summarizes the shear strength equations for stirrup contributions of different design codes. In general, all design models express the shear contribution of stirrup reinforcement as:

$$V_s = \frac{A_v f_{yv} d_v}{s} \cot\theta, \tag{23}$$

where A_v, f_{yv}, and s are the cross-sectional area, tensile yield strength, and spacing of stirrups, respectively; θ is the inclination angle of the diagonal concrete strut, and d_v is the effective shear depth.

As shown in Table 1, the KDS 14 draft model for steel reinforcement adopts the same design equation for stirrup shear contribution as the ACI 318-19. Meanwhile, the CSA A23.3:24 model employs a semi-empirical equation based on the Modified Compression Field Theory (MCFT) to determine θ, differing from the value of 45° used in the ACI and KDS models. In addition, the CSA A23.3:24 provisions included the resistance factors for steel (ϕ_s) and concrete (ϕ_c) in the design equations for V_s and V_c, respectively, to account for uncertainties in material strength. For consistency in evaluation, these resistance factors were set to 1.0. The design model proposed by Marí et al. (2016) accounts for the contribution of stirrup forces intersecting the inclined crack beneath the compression zone.

As shown in Fig. 6a, c, the KDS 14 draft model provided predictive performance comparable to the CSA A23.3:24 and Marí et al. models, with a COV value of 18%, a mean $V_{test}/V_{predict}$ ratio of 1.30 and an AAE of 0.23. For all design models, no specimens exhibited $V_{test}/V_{predict}$ ratios below 0.75. In addition, the $P_{0.05}$ values approached 1.0, indicating high reliability and safety. In comparison with the KDS 14 draft and CSA A23.3:24 models, the ACI 318 model exhibited slightly higher conservatism, with a mean $V_{test}/V_{predict}$ ratio of 1.59 and a COV of 21%.

5 Parametric Study Using Design Models

Fig. 7 presents the results of a parametric study comparing the KDS 14 draft model with existing design models, using selected test series from the ACI-DAfStb database for PSC beams (Muguruma et al., 1983; Elzanaty et al., 1986; Saqan & Frosch, 2009; and De Silva et al., 2006). The influence of the prestressing levels in tendons is shown in Fig. 7a. The normalized prestress (σ_p/f'_c) varied from 0.05 to 0.16, while other design parameters were consistent with those examined by Muguruma et al. (1983). The KDS 14 and ACI 318 models showed good agreement with the test results, demonstrating that the shear strength of PSC beams increases proportionally with prestressing levels. In the KDS 14 draft model, higher prestressing forces led to a greater compression zone depth (Eq. 16) and increased average compressive stress (f_{cc}) in the compression zone (Eq. 15), enhancing overall shear strength. In the ACI 318 model, increased prestressing forces improved the flexural cracking moment (M_{cre}), thereby enhancing the flexure-shear strength (V_{ci}). Conversely, the design concept of CSA A23.3:24 (CSA, 2024) predicted a constant trend of the shear strength, which can be attributed to the limitation in longitudinal strain (ε_x) at the mid-depth of the member.

Fig. 7b, c show that all design models followed the observed increasing trend in shear strength for test series conducted by Elzanaty et al. (1986) as the concrete compressive strength increased, and by De Silva et al. (2006) as the amount of stirrup reinforcement increased. In the KDS 14 draft model, higher compressive strength improved concrete tensile strength, contributing to shear resistance in the compression zone.

Lastly, Fig. 7c presents the parametric results for the test series by Saqan and Frosch (2009), indicating a slight improvement in shear strength with increasing non-prestressed tension reinforcement. The KDS 14 draft model closely aligned with these observations, explicitly accounting for contributions from both non-prestressed and prestressed reinforcement in determining compression zone depth through force equilibrium and strain compatibility (Eqs. 13–16). In contrast, neither the ACI 318 nor CSA A23.3 models consider this effect.

Overall, the parametric study depicted in Fig. 7 indicates that shear strength predictions by the KDS 14 draft model exhibited trends consistent with experimental results in most of the scenarios investigated.

6 Design Example

To understand the KDS design method in the design of the PSC beams, a design example is presented for a post-tensioned beam shown in Fig. 8a. The PSC beam is simply supported and subjected to a uniformly

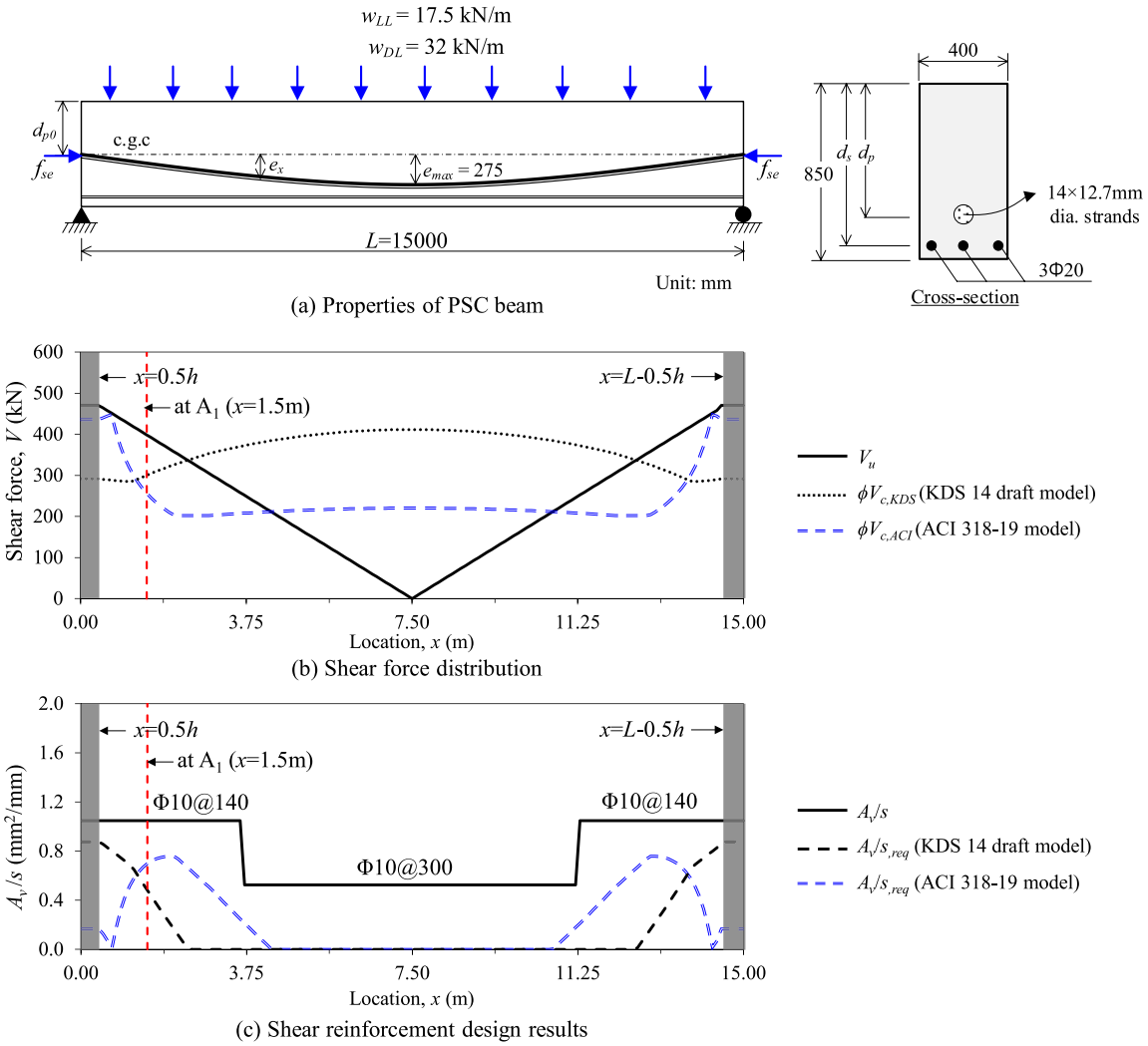

Fig. 8 Shear design example for PSC beam with parabolic strand profile

Table 2 Properties of the PSC beam in design example

Concrete compressive strength	f'_c = 34 MPa
Prestressing steel area	A_p = 1382 mm², E_p = 200,000 MPa
Tensile steel bar area	A_s = 942 mm² (3Φ20), E_s = 200,000 MPa, d_s = 800 mm
Effective prestress	f_{se} = 1000 MPa
Tendon profile and slope at location *x*	$e(x) = -\left(4.89 \times 10^{-6}\right)(x - 7500)^2 + 275 \quad mm$
	$\theta(x) = \left(9.78 \times 10^{-6}\right)x - 0.073 \quad rad$
Span	*L* = 15 m
Dead load (wDL)	w_{DL} = 32 kN/m
Live load (wLL)	w_{LL} = 17.5 kN/m
Section properties	b_w = 400 mm, *h* = 850 mm, d_s = 800 mm, d_{p0} = 425 mm

distributed load. The geometric and material properties of the beam are summarized in Table 2. The beam had a span length of $L=15$ m and cross-sectional dimensions of $b\times h=0.4\times0.85$ m. The bottom longitudinal reinforcement consists of $5\times\Phi25$ bars. The beam is post-tensioned using a parabolic layout tendon, composed by $14\times1/2$" strands with a nominal area of 98.71 mm^2 ($A_p=14\times98.71=1382$ mm^2). The tendon has zero eccentricity at the centroid of the gross cross-section (c.g.c) and reaches its maximum eccentricity at mid-span.

The representative calculation at cross-section $A_1=1.5$ m following the KDS 14 design method is as follows:

- Factored load and internal forces

$$w_u = 1.2w_{DL} + 1.6w_{LL} = 1.2\times32 + 1.6\times17.5 = 66.4\,(\text{kN/m})$$

$$M_u = \left(\frac{Lx}{2} - \frac{x^2}{2}\right)w_u = \left(\frac{15\times1.5}{2} - \frac{1.5^2}{2}\right)66.4 = 672\,(\text{kNm})$$

$$V_u = \left(\frac{L}{2} - x\right)w_u = \left(\frac{15}{2} - 1.5\right)66.4 = 398\,(\text{kN})$$

- Calculation of the compression zone depth

$$P_{p0} = A_p f_{se} = 1.382\times1000 = 1382\,\text{kN}$$

$$E_c = 8500\sqrt[3]{f_c'} = 8500\sqrt[3]{34} = 27,537\,\text{MPa}$$

$$n = \frac{E_s}{E_c} = \frac{200,000}{27,537} = 7.26$$

$$d_p(x=1.5m) = 425 + e(x) = -\left(4.89\times10^{-6}\right)(1500-7500)^2 + 275 + 425 = 524\,\text{mm}$$

$$d = \max\left(0.8h, \frac{A_s d_s + A_p d_p}{A_s + A_p}\right) = \max\left(680, \frac{942\times800 + 1382\times524}{942+1382}\right) = 680\,\text{mm}$$

$$c_u = \left(\frac{P_{p0}}{\varepsilon_c E_c} - n_s A_s - n_p A_p + \sqrt{\left(\frac{P_{p0}}{\varepsilon_c E_c} - n_s A_s - n_p A_p\right)^2 + 2b_w(n_s d_s A_s + n_p d_p A_p)}\right)/b_w$$

$$= \left(\frac{1382\times1000}{0.001\times27,537} - 1382\times7.26 - 942\times7.26 + \sqrt{\left(\frac{1382\times1000}{0.001\times27,537} - 1382\times7.26 - 942\times7.26\right)^2 + 2\times400\times(1382\times7.26\times524 + 942\times7.26\times800)}\right)/400 = 0.329\,\text{m}$$

- Calculation of the compression zone crack angle:

$$M_{ud} = 0.75M_u + P_{p0}(d_p - h/2) = 641\,\text{kNm}$$

$$f_{cc} = \frac{M_{ud} + \left[P_{p0} - A_p\frac{(d_p-c_u)}{c_u}\varepsilon_c E_p\right](d-d_p) - A_s\frac{(d_s-c_u)}{c_u}\varepsilon_c E_s(d-d_s)}{b_w c_u\,(d-c_u/3)}$$

$$= \frac{641\times10^6 + (1382\times10^3 - 1382\frac{(524-329)}{329}0.001\times200,000)(680-524) - 942\frac{(800-329)}{329}0.001\times200,000(680-800)}{400\times329\times(680-329/3)}$$

$$= 11.5\,\text{MPa} \le \frac{2}{3}f_c' = 22.6\,\text{MPa}$$

$$\cot\varphi = \sqrt{1+f_{cc}/f_{te}} = \sqrt{1+11.5/(0.2\sqrt{34})} = 3.295$$

- Calculation of shear contribution by concrete at cross-section A_1:

$$k_s = \sqrt[4]{300/d} = 0.815 \rightarrow 0.75 \le k_s \le 1.1$$

$$V_c = \lambda k_s f_{te} b_w c_u \cot\varphi = 1\,(0.815)(1.17)(0.4)(0.329)(3.295) = 412.6\,\text{kN}$$

$\phi V_c = 0.75 \times 412.6 = 309.5\,\text{kN} < V_u = 398\,\text{kN}$ → Shear reinforcement is required.

- Require $V_{s,req}$:

$$V_{s,req} = V_u - \phi V_c = 398 - 0.75 \times 412.6 = 88.55\,\text{kN}$$

$$\frac{A_v}{s}(req) = \frac{V_u - \phi V_c}{\phi f_{yv} d} = \frac{398 - 0.75 \times 412.6}{0.75 \times 400 \times 680} = 0.44\,\frac{\text{mm}^2}{\text{mm}}$$

Using the same calculation process, the calculation results for the concrete shear contribution (V_c) and the required shear reinforcement for the entire length of the beam are presented in Fig. 8b, c, respectively. According to KDS 14 draft and ACI 318-19 codes, since the critical section of PS beams is usually considered at a distance of 0.5 h from the supports, thus, the calculation results are presented within the region ($0.5\,h \le x \le L - 0.5\,h$).

For comparison, the calculation results using the ACI 318-19 model are presented. In comparison to the ACI 318-19 model, the shear strength evaluated by the KDS 14 draft model is lower in regions subjected to high factored shear force (low factored flexural moment), and higher in regions with low factored shear force. Based on the calculation results, Fig. 8c shows the shear reinforcement layout, consisting of Φ10@100 mm within two lengths of L/4 from the support end and Φ10@150 mm in the remaining span. This arrangement meets the minimum required shear reinforcement ($A_{v,min}$) in accordance with KDS provisions.

7 Conclusion

This study evaluated the predictive capability of the KDS 14 draft design method for determining the shear strength of prestressed concrete (PSC) beams. The assessment utilized the ACI-DAfStb database, which comprises 331 experimental tests on PSC beams with and without shear reinforcement. The performance of the KDS 14 draft model was compared against the ACI 318-19 (ACI, 2019) and CSA A23.3:24 (CSA, 2024) design codes. Additionally, a parametric study and a design example were conducted to examine the influence of critical design parameters and assess the practical applicability of the KDS design approach for PSC beams. The key findings are summarized as follows:

1. The KDS 14 draft model demonstrated strong performance in predicting the one-way shear strength of a large dataset of PSC beams without stirrups. Compared to the ACI 318-19 and CSA A23.3:24 models, it exhibited better accuracy with less scatteredness, achieving a COV value of 20%, a mean shear strength ratio of 1.40, and an AAE of 0.26. The KDS 14 draft model also ensured design conservatism, with a satisfactory safety level indicated by a $P_{0.05}$ value of 0.94 and no specimens exhibiting a $V_{test}/V_{predict}$ ratio below 0.75. The KDS model also exhibited a similar level of scatteredness compared to the mechanics-based model proposed by Marí et al. but provides more conservative predictions.
2. For the dataset of PSC beams with stirrups, the KDS 14 draft model showed predictive performance comparable to the CSA A23.3:24 and Marí et al. models, with a COV value of 18%, a mean $V_{test}/V_{predict}$ ratio of 1.30, and an AAE of 0.23. In comparison, the ACI 318-19 model exhibited slightly higher conservatism than both the KDS 14 and CSA A23.3:24 models.
3. The results of the parametric study using the KDS 14 draft model indicated that the predictions aligned closely with trends observed in experimental results across most scenarios.
4. Based on the compression zone failure theory, the KDS 14 draft model showed that increasing the prestressing level, concrete compressive strength, amount of tension longitudinal reinforcement and stirrups enhanced the overall shear strength of PSC beams. Specifically, higher prestressing levels improved both the compression zone depth and the average compressive stress within the compression zone, contributing to shear resistance. Meanwhile, tension reinforcement mainly affected the compression zone depth. Furthermore, increasing compressive strength improved the tensile strength of the concrete along the critical shear crack, thereby enhancing the shear resistance of the compression zone.

List of symbols

For ACI 318-19

V_{ci}	Flexure-shear strength
V_{cw}	Web-shear strength
f'_c	Concrete compressive strength

b_w and d	Web width and effective depth of the beam, respectively
d_p	Distance from extreme compression fiber to centroid of prestressed reinforcement
V_d	Shear force at section due to unfactored dead load
M_{max}	Maximum factored moment at section due to externally applied loads
V_i	Factored shear force at section due to externally applied loads occurring simultaneously with M_{max}
M_{cre}	Moment causing flexural cracking at section due to externally applied loads
f_{pe}	Compressive stress in concrete due only to effective prestress forces
f_d	Stress due to unfactored dead load
I	Moment of inertia of section about centroidal axis
y_t	Distance from centroidal axis of gross section
F_{pc}	Compressive stress in concrete, after allowance for all prestress losses, at centroid of cross section resisting externally applied loads or at junction of web and flange where the centroid lies within the flange

For CSA A23.3:19

d_v	Effective shear depth
ε_x	Longitudinal strain at mid-depth of the member due to factored loads
A_p	Area of prestressing tendons
f_{po}	Stress in prestressing tendons
M_f, V_f, and N_f	Factored moment, shear force, and axial load, respectively
V_p	Component in the direction of the applied shear of the effective prestressing force
s_{ze}	Equivalent crack spacing parameter
s_z	Crack spacing parameter, s_z shall be taken as d_v or as the maximum distance between layers of distributed longitudinal reinforcement, whichever is less. Each layer of such reinforcement shall have an area at least equal to $0.003\ b_w s$
φ_c and φ_s	Resistance factors for concrete and steel, respectively

For KDS 14

c_u	Depth of the compression zone
f_{cc}	Average compressive stress in the compression zone
$f_{te}[= 0.2\sqrt{f'_c}]$	Concrete tensile strength
k_s	Size effect factor
λ	Reduction factor for lightweight concrete
E_s, E_p, and $E_c[= 8500\sqrt[3]{f'_c}]$	Elastic modulus of steel, prestressed tendons, and concrete, respectively
$P_{p,i}$ and P_{p0}	Prestressing forces in tendons and total prestressing force, respectively
$A_{p,i}$	Cross-sectional area of prestressed tendon
ε_c [= 0.001]	Concrete compressive strain at the extreme compression fiber at the critical section
$d_{p,i}$	Distances between the extreme compression fiber to the centroid of the tendons
A_i	Cross-sectional area of either tensile reinforcement or prestressed tendons; n_i is the modulus ratio between tensile reinforcement/prestressed tendons and concrete
A_v, f_{yv}, and s	Cross-sectional area, tensile yield strength, and spacing of stirrups, respectively
M_u	Factored flexural moment at the design section
M_{ud}	Total applied moment at the design section considering the effect of prestressing force;

For Marí et al. model

ζ	Size effect factor
c and c_0	Neutral axis depth of prestressed and ordinary RC beams, respectively
K_p	Factor which takes into account the effects of prestressing
b and b_w	Width of the flange and web, respectively
$b_{v,eff}$	Effective width
d_s	Distance between the maximum compressed concrete fiber and the centroid of the non-prestressed tensile reinforcement
σ_{cp}	Compression stress at the centroid of the section produced by the prestressing force
f_{ct}	Concrete tensile strength
θ	Strut inclination angle
γ_c	Partial safety factor for concrete

Supplementary Information

The online version contains supplementary material available at https://doi.org/10.1186/s40069-025-00794-0.

Supplementary Material 1.

Acknowledgements
The authors gratefully acknowledge the financial support provided by the Basic Science Research Program of the National Research Foundation of Korea (Grant Nos. NRF-2022R1A2C2004351 and NRF-2020R1A6A1A03044977).

Author contributions
N.H.D: conceptualization, methodology, data curation, writing–original draft. S.-H. K: data curation, investigation. K.-K. C: conceptualization, writing–original draft, review and editing, funding acquisition. All authors read and approved the final manuscript.

Availability of data and materials
The authors declare that the datasets used or analyzed during the current study are available from the corresponding author on reasonable request.

Declarations

Ethics approval and consent to participate
Not applicable.

Consent for publication
Not applicable.

Competing interests
The authors declare no competing interests.

Received: 2 January 2025 Accepted: 10 April 2025
Published online: 13 June 2025

References

AASHTO (American Association of State Highway and Transportation Officials). 2024. AASHTO LRFD Bridge Design Specifications, 10th edition. Washington, DC: AASHTO.
ACI Committee, and International Organization for Standardization, ACI 318-19: *Building code requirements for structural concrete and commentary*. American Concrete Institute, 2019.
CEN (2002) EN1990: Eurocode—basis of structural design. European Commission, Brussels, Belgium.
CSA (Canadian Standard Association), CSA S6:19: *Canadian highway bridge design code*. Ottawa, Canada: CSA Group, 2019.

CSA (Canadian Standard Association), CSA A23.3:24: *Design of Concrete Structures*. Toronto, ON, Canada: CSA Group, 2024.
Chen, W. (1982). *Plasticity in reinforced concrete* (pp. 204–205). McGraw-Hill.
Chen, Y., Wang, C. L., Zeng, B., & Zhu, H. (2024). Design method and experimental investigation of two-stage prestressed precast continuous beams. *Structures, 63*, 106405. https://doi.org/10.1016/j.istruc.2024.106405
Choi, K.-K., Kim, J. C., & Park, H. G. (2016). Shear strength model of concrete beams based on compression zone failure mechanism. *ACI Structural Journal*. https://doi.org/10.14359/51689032
Choulli, Y., Marí, A. R., & Cladera, A. (2008). Shear behaviour of full-scale prestressed i-beams made with self compacting concrete. *Materials and Structures, 41*, 131–141. https://doi.org/10.1617/s11527-007-9225-1
Collins, M. P., Bentz, E. C., Sherwood, E. G., & Xie, L. (2008). An adequate theory for the shear strength of reinforced concrete structures. *Magazine of Concrete Research, 60*(9), 635–650. https://doi.org/10.1680/macr.2008.60.9.635
De Silva, S., Mutsuyoshi, H., Witchukreangkrai, E., & Takagi, M. (2006). Experimental study on shear cracking behavior in I-shaped partially prestressed concrete beams. *Proceedings of the Japan Concrete Institute, 28*(2), 817–822.
Dinh, N. H., Park, S. H., Kim, S. H., & Choi, K. K. (2021). Cyclic behavioral characteristics of RC beams strengthened by U-wrapped TRM jacket with anchorage details. *Engineering Structures, 247*, 113205.
Dunkelberg, D., & Reineck, K. H. (2017). ACI-DAfStb databases 2015 with shear tests for evaluating relationships for the shear design of structural concrete members without and with stirrups. *DAfStb, Germany*.
Elsamak, G., Ghalla, M., Hu, J. W., Albogami, A., Emara, M., & Ahmed, S. O. (2024). Embedded aluminum sections and prestressed high-performance concretes for improving shear performance of RC beams. *Case Studies in Construction Materials, 22*, e04168. https://doi.org/10.1016/j.cscm.2024.e04168
Elzanaty, A. H., & Nilson, A. H. (1986). Shear capacity of prestressed concrete beams using high-strength concrete. *ACI Journal Proceedings, 83*(3), 359–368. https://doi.org/10.14359/10436
Eurocode 2 (EC 2). Design of concrete structures - Part I: General rules and rules for buildings. European Committee for Standardization Brussels; 2002.
fib (Fédération Internationale du Béton): Model Code for Concrete Structures 2010.
Hanson, J. M., & Hulsbos, C. L. (1964). Ultimate shear tests of prestressed concrete i-beams under concentrated and uniform loadings. *Journal of PCI, 9*(256), 15–28.
Hassan, B. R., & Yousif, A. R. (2024). Effect of size factor and tapered angles on the shear behavior and strength of haunched beams reinforced with basalt fiber reinforced polymer rebars: Experimental and analytical study. *Structures, 61*, 106036. https://doi.org/10.1016/j.istruc.2024.106036
Hegger, J., & Görtz, S. (2003). *Analyse des Schubrissverhaltens und dessen Auswirkungen auf die Querkrafttragfähigkeit. Schlussbericht (DBV-Nr. 227)*, Institutsbericht Nr. 86/2003, RWTH Aachen (in German).
Johnson, M. K., & Ramirez, J. A. (1989). Minimum shear reinforcement in beams with higher strength concrete. *ACI Structural Journal, 86*(4), 376–382. https://doi.org/10.14359/2896
Jumaa, G. B., & Yousif, A. R. (2019). Size effect on the shear failure of high-strength concrete beams reinforced with basalt FRP bars and stirrups. *Construction and Building Materials, 209*, 77–94. https://doi.org/10.1016/j.conbuildmat.2019.03.076
Kani, G. N. J. (1964). The riddle of shear failure and its solution. *Journal Proceedings, 61*(4), 441–468. https://doi.org/10.14359/7791
Kar, J. N. (1968). Diagonal cracking in prestressed concrete beams. *Journal of the Structural Division, 94*(1), 83–109. https://doi.org/10.1061/JSDEAG.0001876
KCI (Korea Concrete Institute), KDS 14 20 22: *Design code for shear and torsion of concrete structures*. Ministry of Land, Infrastructure, and Transport of Korea, Seoul, Republic of Korea. (revision draft), 2024.
Kuchma, D. A., Hawkins, N. M., Kim, S. H., Sun, S., & Kim, K. S. (2008). Simplified shear provisions of the AASHTO LRFD bridge design specifications. *PCI Journal, 53*(3), 53–73. https://doi.org/10.15554/pcij.05012008.53.73
Laskar, A., Hsu, T. T., & Mo, Y. L. (2010). Shear strengths of prestressed concrete beams part 1: Experiments and shear design equations. *ACI Structural Journal*. https://doi.org/10.14359/51663698
Leonhardt, F., & Walther, R. (1962). *Schubversuche an einfeldrigen Stahlbetonbalken mit und ohne Schubbewehrung zur Ermittlung der Schubtragfähigkeit und der oberen Schubspannungsgrenze*. W. Ernst & Sohn, Berlin, Germany.
Liu, J., Alexander, J., & Li, Y. (2023). Probabilistic error assessment and correction of design code-based shear strength prediction models for reliability analysis of prestressed concrete girders. *Engineering Structures, 279*, 115664. https://doi.org/10.1016/j.engstruct.2023.115664
Liu, J., Alexander, J., & Li, Y. (2025). Gaussian process regression-based model error diagnosis and quantification using experimental data of prestressed concrete beams in shear. *ASCE-ASME Journal of Risk and Uncertainty in Engineering Systems, Part a: Civil Engineering, 11*(1), 04024095. https://doi.org/10.1061/AJRUA6.RUENG-1455
Marí, A., Bairán, J. M., Cladera, A., & Oller, E. (2016). Shear design and assessment of reinforced and prestressed concrete beams based on a mechanical model. *Journal of Structural Engineering, 142*(10), 04016064. https://doi.org/10.1061/(ASCE)ST.1943-541X.0001539
Megahed, K. (2024a). Prediction and reliability analysis of shear strength of RC deep beams. *Scientific Reports, 14*(1), 14590. https://doi.org/10.1038/s41598-024-64386-w
Megahed, K. (2024b). STM-based symbolic regression for strength prediction of RC deep beams and corbels. *Scientific Reports, 14*(1), 25066. https://doi.org/10.1038/s41598-024-74803-9
Morrow, J., & Viest, I. M. (1957). Shear strength of reinforced concrete frame members without web reinforcement. *ACI Journal Proceedings, 53*(3), 833–869. https://doi.org/10.14359/11558
Muguruma, A.,Watanabe, F., & Fujii, M. (1983). Experimental study on shear resisting behavior of prestressed reinforced concrete beams. *Transactions of the Japan Concrete Institute*, pp. 453–456 (in Japanese).
Muhammad, J. H., & Yousif, A. R. (2023). Effect of basalt minibars on the shear strength of BFRP-reinforced high-strength concrete beams. *Case Studies in Construction Materials, 18*, e02020. https://doi.org/10.1016/j.cscm.2023.e02020
Park, H. G., Choi, K.-K., & Wight, J. K. (2006). Strain-based shear strength model for slender beams without web reinforcement. *ACI Structural Journal, 103*(6), 783. https://doi.org/10.14359/18228
Park, H. G., Kang, S., & Choi, K. K. (2013). Analytical model for shear strength of ordinary and prestressed concrete beams. *Engineering Structures, 46*, 94–103. https://doi.org/10.1016/j.engstruct.2012.07.015
Park, S. H., Dinh, N. H., Kim, S. H., Lee, S. J., & Choi, K. K. (2021). Direct shear behavior of precast panel connections with cast-in-place shear keys using steel fiber-reinforced cementitious mortar (SFRCM). *Structures, 32*, 2130–2142.
Perera, S. V. T., & Mutsuyoshi, H. (2013). Shear behavior of reinforced high-strength concrete beams. *ACI Structural Journal*. https://doi.org/10.14359/51684328
Pham, H. H., Dinh, N. H., & Choi, K. K. (2023). Tensile behavior of lightweight carbon textile-reinforced cementitious composites with dispersed fibers. *Construction and Building Materials, 384*, 131455.
Rupf, M., Ruiz, M. F., & Muttoni, A. (2013). Post-tensioned girders with low amounts of shear reinforcement: Shear strength and influence of flanges. *Engineering Structures, 56*, 357–371. https://doi.org/10.1016/j.engstruct.2013.05.024
Saqan, E. I., & Frosch, R. J. (2009). Influence of flexural reinforcement on shear strength of prestressed concrete beams. *ACI Structural Journal, 106*(1), 60–68. https://doi.org/10.14359/56284
Sozen, M. A., & Hawkins, N. M. (1962). Discussion of "shear and diagonal tension" by ACI-ASCE Committee 326 (426). *ACI Journal Proceedings, 59*(9), 1341–1347.
Tao, X., & Du, G. (1985). Ultimate stress of unbonded tendons in partially prestressed concrete beams. *PCI Journal, 30*(6), 72–91. https://doi.org/10.15554/pcij.11011985.72.91
Taylor, H. P. (1972). Shear strength of large beams. *Journal of the Structural Division, 98*(11), 2473–2490. https://doi.org/10.1061/JSDEAG.0003376
Thoma, S., & Fischer, O. (2023). Experimental investigations on the shear strength of prestressed beam elements with a focus on the analysis of crack kinematics. *Structural Concrete, 24*(4), 4993–5010. https://doi.org/10.1002/suco.202200699
Vecchio, F. J., & Collins, M. P. (1986). The modified compression-field theory for reinforced concrete elements subjected to shear. *ACI Journal, 83*(2), 219–231. https://doi.org/10.14359/10416

Zhang, T., Visintin, P., Oehlers, D. J., & Griffith, M. C. (2014a). Presliding shear failure in prestressed RC beams. I: Partial-interaction mechanism. *Journal of Structural Engineering, 140*(10), 04014069. https://doi.org/10.1061/(ASCE)ST.1943-541X.0000988

Zhang, T., Visintin, P., Oehlers, D. J., & Griffith, M. C. (2014b). Presliding shear failure in prestressed RC beams. II: Behavior. *Journal of Structural Engineering, 140*(10), 04014070. https://doi.org/10.1061/(ASCE)ST.1943-541X.0000984

Zwoyer, E. M., & Siess, C. P. (1954). Ultimate strength in shear of simply-supported prestressed concrete beams without web reinforcement. *ACI Journal Proceedings, 51*(10), 181–200. https://doi.org/10.14359/11673

Publisher's Note

Ngoc Hieu Dinh is a postdoctoral fellow at Soongsil University, Korea. He earned his MS and PhD in Architectural Engineering from Soongsil University. His research interests focus on the seismic design of reinforced concrete (RC) structures and the application of fiber-reinforced concrete and textile-reinforced concrete.

Si-Hyun Kim is a Master's student in the Department of Architecture at Soongsil University, Korea. He received his Bachelor's degree from the School of Architecture at Soongsil University. His research interests include the design and testing of reinforced concrete structures.

Kyoung-Kyu Choi is a Professor of Architectural Engineering at Soongsil University, Korea. He holds a BE, MS, and PhD in Architectural Engineering from Seoul National University. He is a former associate member of the Joint ACI–ASCE Committee 445 and a two-time recipient of the ACI Chester Paul Siess Award for Excellence in Structural Research (2009 and 2012). His research interests include the shear and seismic design of RC structures and the application of fiber-reinforced concrete.